

# Three-dimensional Composite Lattice Structures Fabricated by Electrical Discharge Machining

J. Xiong · B. Wang · L. Ma · J. Papadopoulos · A. Vaziri · L. Wu

Received: 25 November 2012 / Accepted: 26 August 2013 / Published online: 10 October 2013  
© Society for Experimental Mechanics 2013

**Abstract** We present a novel method for fabricating carbon fiber composite sandwich panels with lattice core construction by means of electrical discharge machining (EDM). First, flat-top corrugated carbon fiber composite cores were fabricated by a hot press molding method. Then, two composite face sheets were bonded to each corrugated core to create precursor sandwich panels. These panels were transformed into sandwich panels with near-pyramidal truss cores by EDM plunging-cutting the corrugated core between the face sheets with a shaped cuprite electrode. The flat top corrugation permits adhesive to be applied consistently, and the selected dimensions leave a substantial bond area after cutting, resulting in a strong core-to-sheet bond. The crushing behavior of this novel construction was investigated in flatwise compression, and the results were compared to analytical expressions for strength and stiffness.

**Keywords** Carbon fiber · Lattice structures · Sandwich panel · Mechanical properties · Electrical Discharge Machining

## Introduction

Sandwich panels assembled of skins and cores have been widely used in naval and aeronautical applications since they offer high specific stiffness and strength [1], as well as high

impact tolerance and blast resistance [2–4]. The core construction plays a critical role in the overall performance of these panels [5]. Truss-like lattice structures are attractive alternatives to honeycomb and folded plate cores as they provide unique multifunctional advantages [6, 7]. Emergence of novel manufacturing techniques in recent year has allowed fabrication of lattice structures from metallic alloys [8–12] and more recently fiber reinforced composites [13–19]. An example is the work of Finnegan et al. [16], where composite pyramidal truss cores were manufactured by water-jet cutting to create snap-fitting joints and It is clear that topologically structuring composite materials show promise for filling gaps in the strength versus density map of all known materials. Wang et al. [17] and Xiong et al. [18] fabricated carbon fiber composite pyramidal truss cores using a hot press molding technique on continuous slender ribbons of prepreg. Liu et al. [19] investigated the mechanical properties and failure mechanisms of carbon fiber composite sandwich panels with pyramidal truss cores subjected to temperatures ranging from  $-100$  °C to  $350$  °C. These were bonded to flat composite sheets to build ‘all composite’ sandwich panels with pyramidal lattice truss cores. Under out of plane shear forces these sandwich panels generally fail prematurely at pyramid apexes due to the small area of bond to the face sheets, and thus do not achieve the theoretical core-limited strength. In this paper, we used electrical discharge machining (EDM)—previously used to transform corrugated metallic core into a truss structure [20]—to fabricate a carbon fiber composite sandwich panel with a three-dimensional lattice core structure. The principle of electric discharge machining (using a proprietary system developed at Harbin Institute of Technology) is shown in Fig. 1. A key challenge in the application of EDM to carbon fiber composites is the low electrical conductivity of the composite material [21]. To address this challenge we used cuprite cutting electrodes, enhanced the composite structure’s conductivity, and systematically adjusted the EDM processing

---

J. Xiong (✉) · B. Wang · L. Ma (✉) · L. Wu  
Center for Composite Materials and Structures, Harbin Institute of Technology, Harbin 150001, People’s Republic of China  
e-mail: xiongjian0309@126.com  
e-mail: mali@hit.edu.cn

J. Xiong · J. Papadopoulos · A. Vaziri  
Department of Mechanical and Industrial Engineering, Northeastern University, Boston, MA 02115, USA



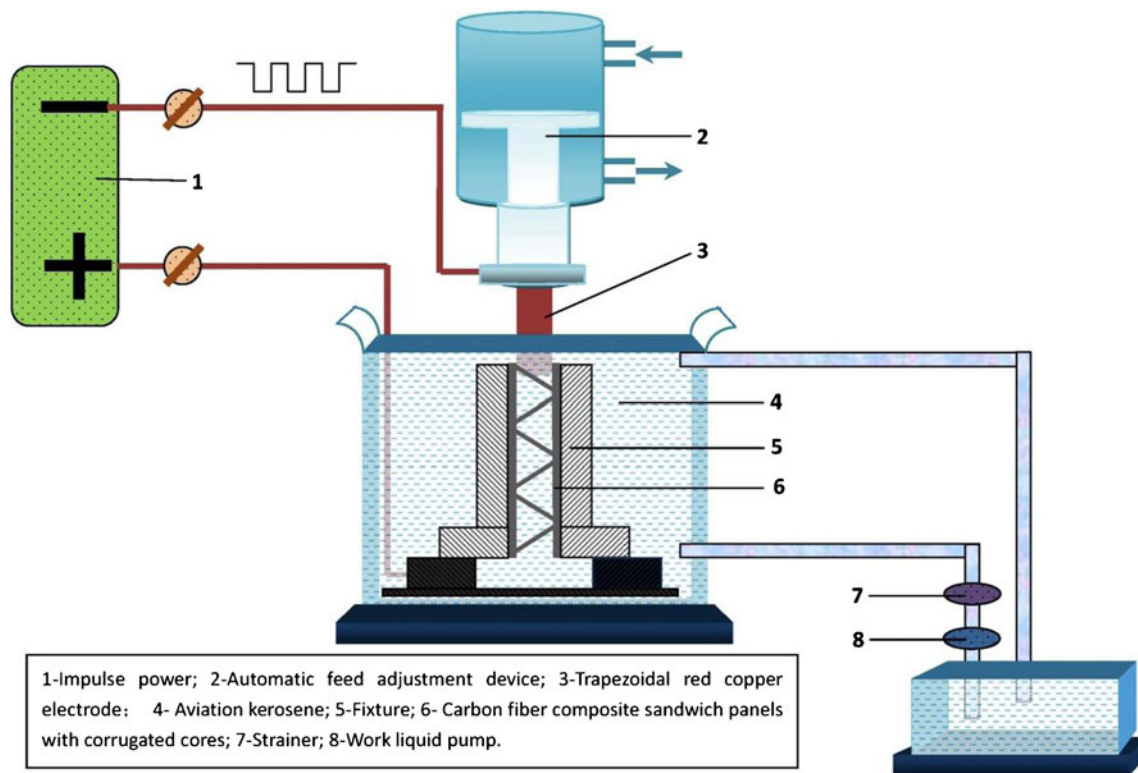


**Fig. 1** Schematic of the electrical discharge machining equipment developed at Harbin Institute of Technology

parameters to optimize cutting of thin-wall carbon fiber composite structures. We applied this method to transform carbon-fiber composite sandwich panels with corrugated core into sandwich panels with lower-density, near-pyramidal, truss-like cores. Details of our fabrication method are presented in “Materials and Fabrication”. In “Out-of-Plane Compression Test”, “Analytical Models for Compressive Stiffness and Failure” and “Results and Discussion”, we describe the crushing behavior and compare the experimental results to the analytical predictions. Conclusions are drawn in “Conclusion”.

## Materials and Fabrication

Carbon fiber composite corrugated cores were laminated from 0.15 mm thick unidirectional carbon fiber/epoxy prepreg sheets. The as-cured mechanical properties (supplied by the manufacturer, Beijing Institute of Aeronautical Materials) are provided in Table 1. Unidirectional prepreg was chosen because its high volume fraction of fibers (about 60 %) was needed to maximize electrical conductivity for the EDM process. The corrugated core was manufactured with fiber orientations  $[-35^\circ/+35^\circ/-35^\circ/+35^\circ/-35^\circ/+35^\circ]$  by the hot-press molding method, where the angle  $35^\circ$  is chosen to align half of the fibers with struts formed by cutting at similar in-plane angles—of course, this layup is not as light as strut construction from continuous fiber ribbons. During core fabrication,

0.5 MPa average pressure and  $120^\circ\text{C}$  temperature were applied by mating corrugated dies (with additional parting-paper fillers used to maintain gap uniformity, when separating the dies to fabricate thicknesses greater than 0.9 mm). The flat-top corrugations permit adhesive to be applied more consistently, and the selected dimensions provide a large core-to-sheet bond area, resulting in a strong core-to-sheet bond.

These corrugated cores were transformed into truss-like cores by EDM plunge-cutting with a multi-prong shaped

**Table 1** Properties of unidirectional laminate (T700/epoxy composites)

Properties	Value
0°Tensile strength (MPa)	1400
0°Tensile modulus (GPa)	123
0°Compression strength (MPa)	850
0°Compression modulus (GPa)	100
90°Tensile strength (MPa)	18
90°Tensile modulus (GPa)	8.3
90°Compression strength (MPa)	96
90°Compression modulus (GPa)	8.4
In-plane shear strength (MPa)	16.0
In-plane shear modulus (GPa)	4.8
Interlayer shear strength (MPa)	60
Major Poisson's ratio	0.3
Volume fraction of fibers	57 % $\pm$ 3

cuprite electrode. We envisioned two convenient ways to cut a corrugated core, shown schematically in Fig. 2: In the first method, cutting is performed prior to bonding between face sheets, by an alternating pattern of triangular-shaped EDM electrodes translating axially in a direction normal to the plane of the future sandwich panel. The end of each electrode is inclined parallel to the sloped face of the corrugated core in order to improve the cutting efficiency. Face sheets are bonded to the core after it is cut, and is in a less-rigid condition. In the second method, two flat composite sheets are first bonded to a corrugated core to create a precursor “corrugated core” sandwich panel. A row of EDM electrodes can be designed to cut all the holes horizontally, i.e. parallel to the face sheets.

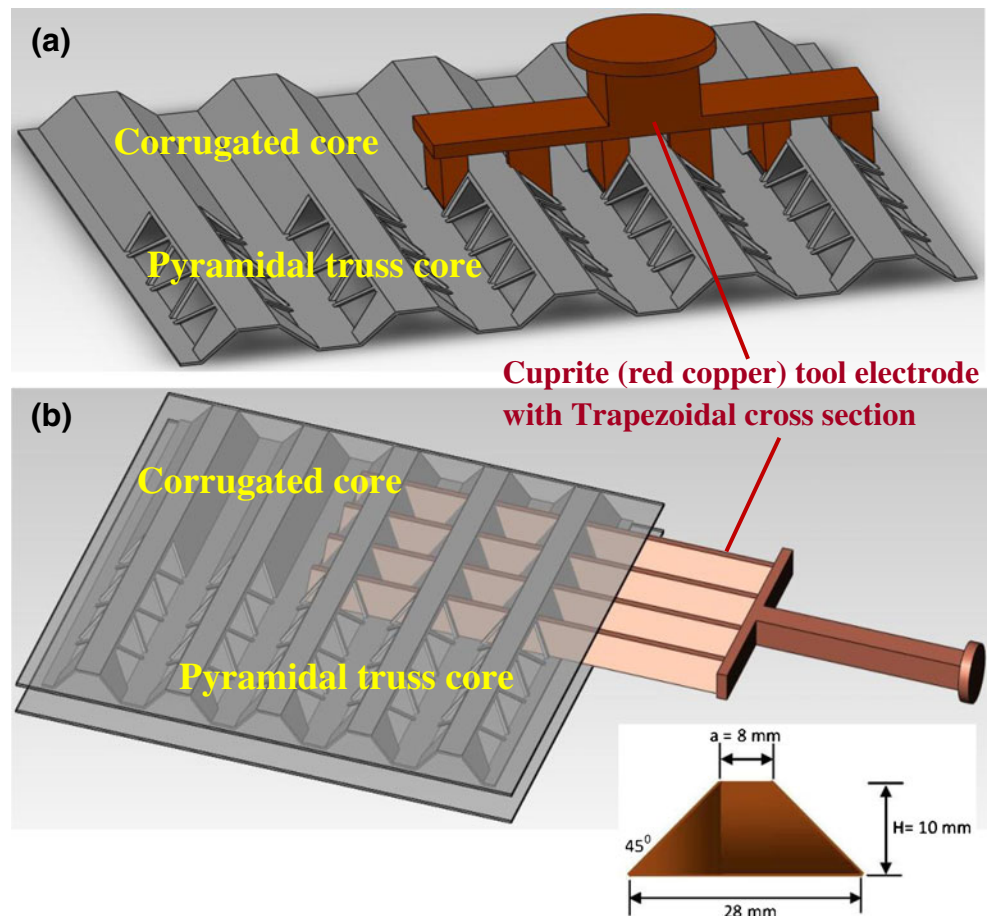
For this investigation, we used the second method to cut the corrugated cores. Carbon fiber reinforced face sheets with the ply sequence of  $[-45^\circ/45^\circ/90^\circ/0^\circ/0^\circ/90^\circ/45^\circ/-45^\circ]$  were bonded to the corrugated core with epoxy adhesive (08–57, Heilongjiang Petrochemical Institute). Face sheets are needed to support corrugated or truss-like core for testing, but the specific sheet properties are expected to have little influence on the measured core strength and stiffness. Since electrical conduction to the core is impeded by the adhesive joining it to the face sheets, we connected

copper wire between the face sheet and the corrugated core at each corner of the panel.

The bonded sandwich panels were soaked in aviation kerosene to increase cutting speed and reduce electrode wear. Taghavi et al. [22] investigated the effect of kerosene on the interface of the unidirectional composites and found that it was unaffected even after 3,500 h of 80 °C kerosene immersion. Based on the results of this work, we assumed that the influence of kerosene immersion on the properties of fiber reinforced composite is minimal. It is emphasized that we have not examined this effect in the current study.

A range of process parameters was tested and the following parameters were selected: processing current 0.5–5.0 A, discharge voltage 10 V, pulse duration 80–550  $\mu\text{s}$ , pulse separation 120–550  $\mu\text{s}$ . These settings result in an effective and repeatable manufacturing process. The average electrode penetration rate into the corrugated core was about 1.5 mm/min, so even with many electrodes cutting simultaneously from both edges, the machining of a panel of 1.5 m width would take hours. Thin-walled hollow electrodes would reduce the amount of material to be eliminated, and thus increase the cutting speed. Furthermore, in principle it would be possible to use hundreds of long electrodes (one within each corrugation trough), each

**Fig. 2** Schematic illustration of the trapezoidal regions removed from the corrugated core by electrical discharge machining (EDM) to create a carbon fiber composite pyramidal truss-like core. (a) The first method-sloped tool end: from *top* to *bottom* without bonded face sheets. (b) The second method-vertical tool end: from *right* to *left* with bonded face sheets. (The pictured tools must be rotated or translated to produce adjacent, i.e. inverted, trapezoidal holes.) The dimensioned shape is a vertical cross section of the horizontal tool



able to cut hundreds of holes simultaneously in 1.5 mm of transverse motion. Thus all holes in a panel could perhaps be cut in a few minutes—a cost-effective transformation not possible with the laser cutting method.

The resulting core unit cells are shown in Fig. 3(a). By design, the process results in a truss-like arrangement in which struts do not quite meet at common nodes. This is done to enlarge the core-sheet bonding area compared to a pyramidal truss core, and to allow the application of adhesive along the core corrugation tops to be simpler and more reliable. The relative densities (i.e., volume fraction) of corrugated core (=cc), and near-pyramidal, cut-from-corrugated truss core (=pc), are given by:

$$\bar{\rho}_{cc} = \frac{2t \left( 2b + h / \sin\theta - t \tan \frac{\theta}{2} \right)}{L(h+t)} \quad (1)$$

$$\bar{\rho}_{pc} = \frac{2tW \left[ (h-H) / \sin\theta - t \tan \frac{\theta}{2} \right] + 4tbW + 4tH / (\sin\theta \cos\alpha)}{WL(h+t)} \quad (2)$$

The dimensions  $a$  and  $H$  are shown in Fig. 2(b), and  $b$ ,  $d$ ,  $h$ ,  $t$ ,  $\theta$ ,  $\alpha$ ,  $\omega$  are shown in Fig. 3(a). The angle  $\omega$  in equations (1) and (2) is calculated from  $\sin(\omega) = \sin(\theta) \cos(\alpha)$ . The electrode sidewall angle  $\beta$ , shown as  $45^\circ$  in Fig. 2(b), can be found from  $\tan(\beta) \tan(\alpha) = \sin(\theta)$ . Note,  $d$  is measured perpendicular to a strut, not horizontally.  $L = 4b + 2h / \tan\theta - 2t \tan \frac{\theta}{2}$  is the corrugation wavelength from trough to trough, and  $W = 2a + 2d / \cos\alpha + 2H \tan\alpha / \sin\theta$  is the width of a single ‘pyramidal cell’ along the corrugation ridge direction. Figure 3(b) shows a photograph of the resulting lattice sandwich structure. The samples manufactured here have  $t=0.9$  mm,  $a=8$  mm,  $b=4.75$  mm,  $d=4$  mm,  $h=12$  mm,  $H=10$  mm,  $\theta=45^\circ$ ,  $\beta=45^\circ$ ,  $\alpha=35.2^\circ$  (to nearly match the core sheet fiber angle of  $35^\circ$ ), and therefore also  $\omega=35.2^\circ$ , resulting in a computed relative density of approximately 4.95 %. The relative density of the precursor corrugated core was about 8.62 %. To put this in

perspective, note that consolidating the core into a uniform flat sheet would give a thickness of  $(h+t)\rho_c = (12+0.9)(.0495) = 0.64$  mm. With face sheets of 1.2 mm thickness, the core accounts for just 21 % of total panel mass but 84 % of the volume.

Several struts were detached from the specimen to evaluate the effect of EDM on the strut surface. Figure 4 shows an SEM image of a strut edge formed by EDM cutting. The lower part shows the as-molded surface, and plunge cutting occurred normal to the image at the top dashed line. For a distance of about 15–20  $\mu\text{m}$  below the cut surface, the fibers were strongly affected and the epoxy matrix was almost fully removed due to the high local temperatures. Down to 50  $\mu\text{m}$  below the cut (bottom dashed line), a small amount of epoxy matrix was removed. In the bottom third of the micrograph, debris makes it difficult to estimate the erosion depth on the front surface. However, we surmise that the damage depth away behind the illustrated face could be significantly less than 50  $\mu\text{m}$ . Based on our observation, EDM produces a better quality and more precise surface compared to laser cutting. With the present electrodes and equipment, EDM cutting of the core to create struts is slower than laser cutting. As an example, a pyramidal lattice core with  $3 \times 3$  unit cells was EDM-cut in 8 h with one electrode, compared with laser cutting in 0.5 h. However, the speed of manufacturing can possibly be increased significantly by redesigning the electrodes to cut all the bonded-panel holes simultaneously, and then EDM should be much faster than the laser cutting method. To explore this approach with full-size panels will require a larger EDM workspace.

### Out-of-Plane Compression Test

Using a screw-driven testing machine (INSTRON 5569), we carried out flatwise compression tests on the panel samples based on ASTM C365/C 364M-05, ‘Standard Test Method for Flatwise Compressive Properties of Sandwich Cores’ [23]. Face sheets are required for this measurement, since unlike

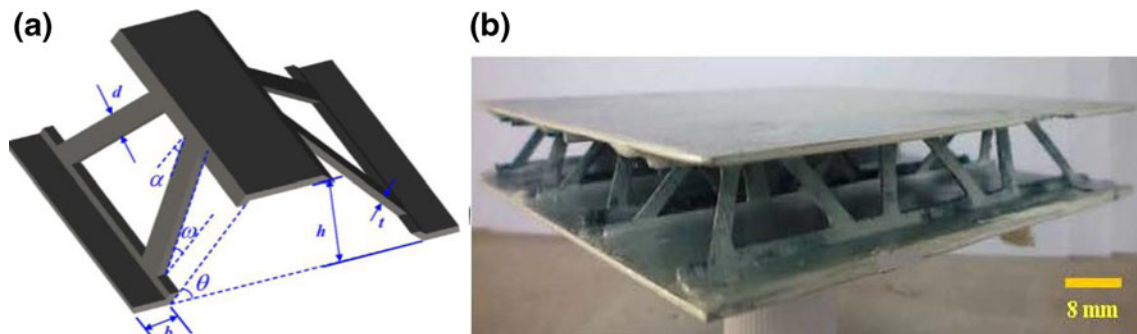


**Fig. 3** (a) Schematic image of the unit cell of pyramidal truss-like core produced by electrical discharge machining similar to the unit cell in a previous paper [26]. Note that  $t$  is uniform,  $h$  is to the underside of the top surface,  $\alpha$  is measured in the plane of the sloping sidewall,  $\omega$  is an elevation angle relative to a horizontal plane, and  $b$  is measured on the exterior face of the top and bottom surfaces. (b) Photograph of an EDM carbon fiber composite pyramidal truss-like core sandwich structure. The core relative density is calculated to be 4.95 %

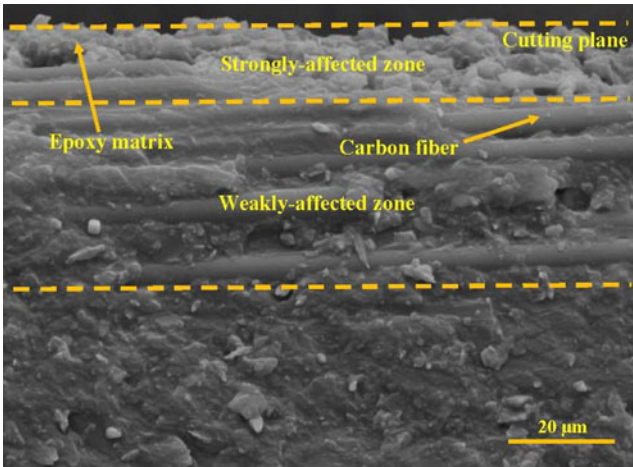


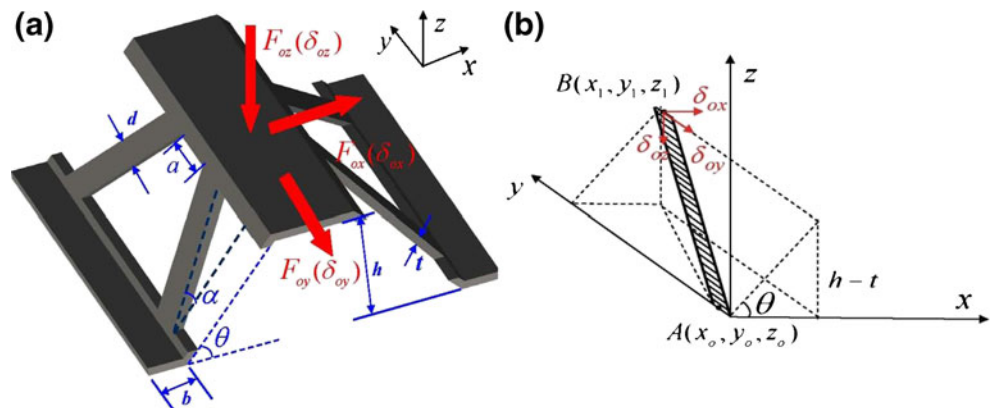
**Fig. 4** A scanning electron microscope (SEM) image of damage from EDM processing. The imaged face is a molded surface that was cut in a direction ‘into’ the paper at the top dashed line. EDM damage below a 50 μm depth appears slight, and behind this front molded face might have penetrated even less

traditional honeycomb cores, a truss-like core must be bonded to prevent spreading and develop its full *in situ* buckling resistance. The specimens used in this set of experiments were three pyramids wide by three pyramids long (total of 9 unit cells) with overall dimensions of 45.8 mm (width) × 42.3 mm (length). The applied load was measured by load cell in the INSTRON 5569, while a laser extensometer (Epsilon) was used to measure the nominal compressive strain. The compression tests were carried out in the quasi-static regime with a nominal displacement rate of 0.5 mm/min at room temperature. An unloading-reloading curve (dotted) was used to determine the effective elastic modulus near peak load. Three tests were conducted.

**Analytical Models for Compressive Stiffness and Failure**

In this section, analytical models for the flatwise crushing response of pyramidal truss-like cores were developed by

**Fig. 5** (a) Unit cell of a oblique pyramidal truss-like core subjected to compressive and shear loading [26]. (b) Geometry of a single strut



analyzing the elastic deformation of a single strut of a pyramidal truss-like core. The stiffness model is based on both axial and flexural stiffness of the core struts [24, 25]. The strength models are based on the axial loads applied to each strut when the panel is subjected to a flatwise (i.e., through-thickness) compressive load. Euler buckling and compressive fracture of the composite struts are the two competing failure modes. The framework for analysis of individual struts of a pyramidal-like core with oblique strut morphology is shown in Fig. 5.

Because of geometric symmetry, loads along any coordinate axis will result in displacement along that axis. Therefore, compressive calculations can be made by considering displacement purely along the  $z$  coordinate direction, where each of the four struts contributes exactly one fourth of the total stiffness. To determine the angles and length of a strut, a coordinate system is placed at the lower end A, and relative coordinates of the upper end, B, are found:

$$\text{For } A(x_o, y_o, z_o), x_o = y_o = z_o = 0;$$

$$\text{For } B(x_1, y_1, z_1), x_1 = l \cos \theta,$$

$$y_1 = l \sin \theta \sqrt{\csc^2 \theta \sec^2 \alpha - 1 - \cot^2 \theta}, z_1 = l \sin \theta.$$

The length of the single strut  $l_{AB}$  and the deformation of the single strut  $\Delta l_{AB}$  are found as follows:

$$l_{AB} = \sqrt{(x_1 - x_o)^2 + (y_1 - y_o)^2 + (z_1 - z_o)^2} = l \sec \alpha \tag{3}$$

$$\Delta l_{AB} = [\delta_x \quad \delta_y \quad \delta_z] \begin{bmatrix} \frac{x_1 - x_o}{l_{AB}} & \frac{y_1 - y_o}{l_{AB}} & \frac{z_1 - z_o}{l_{AB}} \end{bmatrix}^{-1} \tag{4}$$

$$= \delta_x \frac{x_1 - x_o}{l_{AB}} + \delta_y \frac{y_1 - y_o}{l_{AB}} + \delta_z \frac{z_1 - z_o}{l_{AB}}$$

Analytical models for flatwise stiffness and strength of these truss-like cores cut from corrugated cores were developed by methods similar to those presented in [26]. The results are summarized below.

The effective Young’s modulus of the pyramidal truss-like structure can be estimated from,

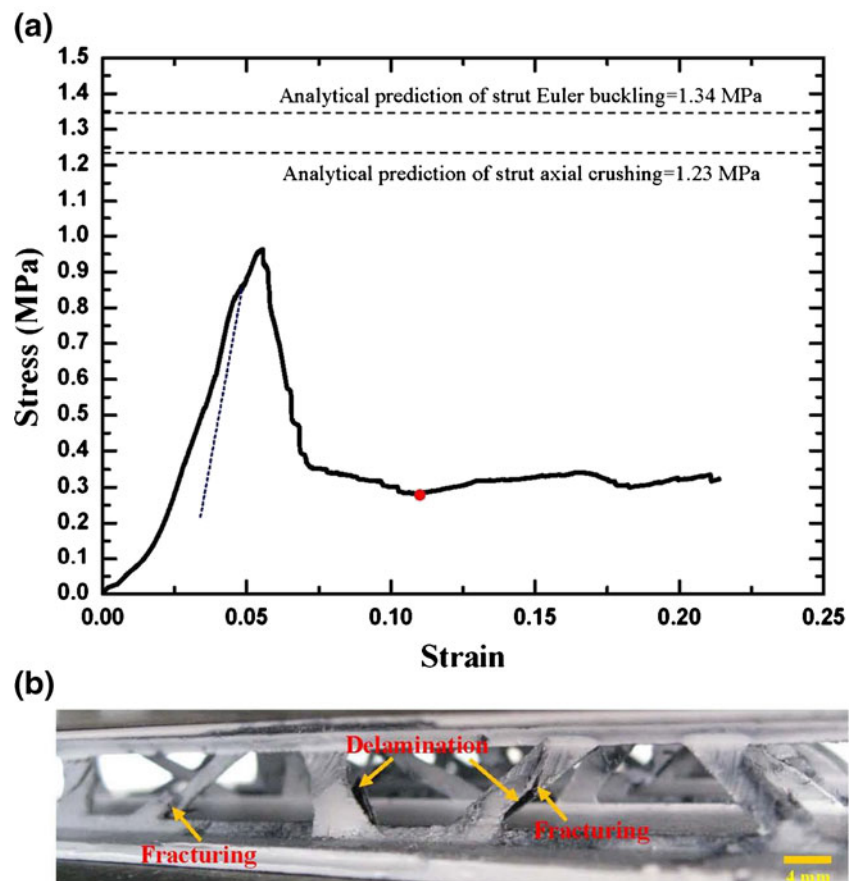
**Table 2** Calculated and measured results for the compressive stiffness and strength of pyramidal truss-like core sandwich structure with core relative density 4.95 %

Mechanical properties		Calculated (MPa)	Measured (MPa)
Compressive stiffness		65.05	30.28
			34.90±3.44
			35.89
Compressive strength	Euler buckling	1.34	0.91
	crushing	1.23	0.95
			1.01
			0.96±0.04
		(All from crushing)	

While the core was laminated as  $[35^\circ/-35^\circ/35^\circ/-35^\circ/35^\circ/-35^\circ]$ , adequate samples were not available for testing. Therefore, fiber-direction properties needed for strut-axial calculations were simply estimated from  $0^\circ$  compressive testing of the relatively similar (i.e., half of the fibers roughly perpendicular) 24-layer laminate  $[0^\circ/90^\circ/0^\circ/90^\circ/0^\circ/90^\circ]_4$ . Therefore, the unloading modulus was found as  $E_{cc}=34.3\text{ GPa}$ , which may be contrasted with 100 GPa for unidirectional composite with optimal fabrication conditions. The fiber-direction compressive delamination strength is  $\sigma_{cc}=278.8\text{ MPa}$  (contrasted with 850 MPa for unidirectional composite)

$$E_{Eq} = \frac{E_{cc}dt(h+t)\sin^3\omega \left[ 1 + \left( \frac{d\sin\omega\sin\theta}{H} \right)^2 \right]}{H \left[ h/\tan\theta + 2b - t \tan \frac{\theta}{2} \right] \left[ a + \frac{H\tan\alpha}{\sin\theta} + \frac{d}{\cos\alpha} \right]} \quad (5)$$

**Fig. 6** Flatwise compressive behavior of a panel sample: (a) Macroscopic stress versus macroscopic strain curve, schematically indicating an elastic unloading-reloading line for modulus determination (dotted). (b) Photograph of core failure mechanisms (compressive delaminating and fracturing) taken at the point on the stress-strain curve marked by a red dot



Two failure mechanisms for the core struts under flatwise compression are elastic buckling and crushing (including fracture and delamination). The analytical models for predicting the failure stress associated with each failure mechanism are derived as

$$\sigma_E = E_{eq} \frac{\pi^2}{3} \frac{t^2}{H(h+t)} \quad (\text{strut buckling}) \quad (6)$$

$$\sigma_{cf} = \sigma_{cc} \left( \frac{E_{eq}}{E} \right) \left( \frac{H}{h+t} \right) \frac{1}{\sin^2\omega} \quad (\text{strut crushing}). \quad (7)$$

Values for the geometric parameters were provided in the paragraph following equation (2), above.  $E_{eq}$  is the equivalent (macroscopic) core compressive modulus, and  $\sigma_E$  is the macroscopic stress for strut Euler buckling, so equation (6) implies that buckling occurs at a critical value of the compressive strain.  $\sigma_{cf}$  is the macroscopic stress for strut compressive crushing or delamination failure, and estimates for the corrugated core in-plane strength  $\sigma_{cc}$  and stiffness  $E_{cc}$  are given in Table 2. Since the  $+35^\circ/-35^\circ$  fiber orientations in the core sheets were nearly perpendicular, we simply used the in-plane compressive properties along the  $0^\circ$  direction of  $[0^\circ/90^\circ/0^\circ/90^\circ/0^\circ/90^\circ]$  flat sheets, measured according to the ASTM D664.

## Results and Discussion

Figure 6(a) shows a typical compressive stress-strain response. Disregarding an initial phase (approximately 0.015 strain) of developing load-bearing contact and failing some locally overloaded epoxy, the initial response of the structure is quite linear. This is followed by a small nonlinear regime of degraded stiffness due to the onset of compressive delamination/fracture of struts. After reaching a peak load, a series of local failure events lead to a reduction in strength, see Fig. 6(b). No bond failures occurred during these compression experiments.

Calculated stiffness and strength estimates are compared to measured results in Table 2, where it is seen that the predicted strut crushing failure strength (1.23 MPa) is slightly lower than the predicted strut-buckling strength (1.34 MPa). The mean measured core stiffness is 46 % lower and mean measured peak strength is 22 % lower than calculated. We speculate that the stiffness deviation could be due to imperfect specimen-to-platen contact (since platens were not self-aligning), and the strength deviation could be due to mold pressure and temperature inconsistencies during core fabrication. The damage depth from EDM is about 50  $\mu\text{m}$ , much smaller than the 400  $\mu\text{m}$  damage caused by laser cutting. Therefore, the mechanical properties of EDM-cut core can be expected to exceed those of laser cut core with the same nominal dimensions. Indeed, the flatwise compressive strength of a panel with EDM-cut core is about 5 % greater than that with laser-cut core [26]. Since EDM forms slender members with greater strength, it may be preferred for millimeter scale structures.

## Conclusion

Fiber reinforced composite structures with lattice truss topologies appear to offer one of the highest specific strengths of all low density (i.e., high void-fraction) materials. Here, we adapted the EDM method of metal cutting to the high-precision cutting of carbon fiber composite, to permit the conversion of a corrugated core sandwich panel into a truss core sandwich panel. The dimensions of the precursor corrugated core, and of the cutting tool, resulted in a far greater bond area, and possibly a more reliable adhesive application to the core. On the other hand, core density is greater than for some other configurations, since there is a large ‘top’ area, and the struts have only half of their fibers in the axial direction. Flatwise panel compression was conducted to understand the mechanical properties and crushing behavior, and fair agreement between the measurements and predictions was obtained. The enlarged core-to-face-sheet bond area could plausibly suppress the kinds of failures previously observed in shear loading; this will be investigated in future.

**Acknowledgments** The present work was supported in part by the Major State Basic Research Development Program of China (973 Program) under grant No. 2011CB610303, National Science Foundation of China under grant Nos. 11222216, 11302060 and the Fundamental Research Funds for Central Universities under Grant No. HIT.BRETIV.201301. AV and JP acknowledge the support by the U.S. Air Force Office of Scientific Research under AFOSR YIP grant award, #FA 9550-10-1-0145 and technical direction of Dr. Joycelyn Harrison. JX also gratefully acknowledges support by the Natural Sciences Research Innovation Foundation in Harbin Institute of Technology (HIT.NSRIF.2014025) and Open-ended fund of Science and Technology on Advanced Composites in Special Environments Laboratory.

## References

- Ravichandran G, Rajapakse YDS (2012) Sandwich structures. *Exp Mech* 52:1–2
- Ebrahimi H, Vaziri A (2013) Metallic sandwich panels subjected to multiple intense shocks. *Int J Solids Struct* 50(7–8):1164–1176
- Mori LF, Lee S, Xue Z, Vaziri A, Queheillalt DT, Dharmasena KP, Wadley HNG (2007) Deformation and fracture modes of sandwich structures subjected to underwater impulsive loads. *J Mech Mater Struct* 2(10):1981–2006
- Wadley HNG, Dharmasena KP, Queheillalt DT, Chen YC, Dudd P, Knight D (2007) Dynamic compression of square honeycomb structures during underwater impulsive loading. *J Mech Mater Struct* 2(10):2025–2048
- Vaziri A, Xue Z, Hutchinson JW (2007) Metal sandwich plates with polymer foam-filled cores. *J Mech Mater Struct* 1(1):97–127
- Lu TJ, Valdevit L, Evans AG (2004) Active cooling by metallic sandwich structures with periodic cores. *Prog Mater Sci* 50:789–815
- Valdevit L, Pantano A, Stone HA, Evans AG (2006) Optimal active cooling performance of metallic sandwich panels with prismatic cores. *Int J Heat Mass Transf* 49:3819–3830
- Ashby MF, Brechet YJM (2003) Designing hybrid materials. *Acta Mater* 51:5801–5821
- Mori LF, Queheillalt DT, Wadley HNG, Espinosa HD (2009) Deformation and failure modes of I-Core sandwich structures subjected to underwater impulsive loads. *Exp Mech* 49:257–275
- Lu TJ, Zhang QC (2010) Novel strengthening methods for ultralightweight sandwich structures with periodic lattice cores. *Sci China Technol Sci* 53(3):875–877
- Zhang QC, Han YJ, Chen CQ, Lu TJ (2009) Ultralight X-type lattice sandwich structure (I): concept, fabrication and experimental characterization. *Sci China Technol Sci* 52(8):2147–2154
- Zhang QC, Chen AP, Chen CQ, Lu TJ (2009) Ultralight X-type lattice sandwich structure (II): Micromechanics modeling and finite element analysis. *Sci China Technol Sci* 52(9):2670–2680
- Park S, Russell BP, Deshpande VS, Fleck NA (2012) Dynamic compressive response of composite square honeycombs. *Compos Part A* 43:527–536
- Russell BP, Deshpande VS, Wadley HNG (2008) Quasistatic deformation and failure modes of composite square honeycombs. *J Mech Mater Struct* 3:1315–1340
- Lee BC, Lee KW, Byun JH, Kang KJ (2012) The compressive response of new composite truss cores. *Compos B* 43:317–324
- Finnegan K, Kooistra G, Wadley HNG, Deshpande VS (2007) The compressive response of carbon fiber composite pyramidal truss sandwich cores. *Int J Mater Res* 98:1264–1272
- Wang B, Wu LZ, Ma L, Sun YG, Du SY (2010) Mechanical behavior of the sandwich structures with carbon fiber-reinforced lattice truss core. *Mater Des* 31:2659–2663

18. Xiong J, Ma L, Wu LZ, Wang B, Vaziri A (2010) Fabrication and crushing behavior of low density carbon fiber composite pyramidal truss structures. *Compos Struct* 92:2695–2702
19. Liu JY, Zhou ZG, Wu LZ, Ma L (2012) A study on mechanical behavior of carbon fiber composite sandwich panel with pyramidal truss cores at different temperatures. *Sci China Phys Mech Astron* 55(11):2135–2142
20. Queheillalt DT, Murty Y, Wadley HNG (2008) Mechanical properties of an extruded pyramidal lattice truss sandwich structure. *Scr Mater* 58:76–79
21. Lau WS, Wang M, Lee WB (1990) Electrical discharge machining of carbon fiber composite materials. *Int J Mach Tool Manuf* 30:297–308
22. Taghavi SG (2000) Moisture effects on high performance polymer composites. Master Dissertation. Department of Chemical Engineering and Applied Chemistry. University of Toronto
23. ASTM: C365/C 364M-05 standard test method for flat wise compressive properties of sandwich cores, ASTM Int. West Conshohocken, PA, 2006
24. Kazemahvazi S, Tanner D, Zenkert D (2009) Corrugated all-composite sandwich structures. Part I: modeling. *Compos Sci Technol* 69:913–919
25. Kazemahvazi S, Tanner D, Zenkert D (2009) Corrugated all-composite sandwich structures. Part II: failure mechanisms and experimental programme. *Compos Sci Technol* 69:920–925
26. Xiong J, Ma L, Vaziri A, Papadopoulos J, Wu LZ (2012) Mechanical behavior of carbon fiber composite lattice core sandwich panels fabricated by laser cutting. *Acta Mater* 60(13–14):5322–5334